High-pressure melting curve of platinum from *ab initio* Z method

A. B. Belonoshko and A. Rosengren
Condensed Matter Theory, Theoretical Physics, AlbaNova University Center, KTH Royal Institute of Technology, SE-106 91 Stockholm, Sweden
(Received 22 February 2012; published 7 May 2012)

Pt is widely used as a standard in high-pressure high-temperature experiments. The available experimental and theoretical data on Pt thermal stability is not consistent. We address the issue of high-pressure Pt melting by *ab initio* molecular dynamics. We demonstrate a remarkable consistency of our computed melting curve with the experimental data by N. R. Mitra, D. L. Decker, and H. B. Vanfleet [Phys. Rev. **161**, 613 (1967)]. The extrapolation of their data, based on the Simon equation, nearly coincides with our *ab initio* computed melting curve. We propose the Pt melting curve in the form $P_m(\text{kbar}) = 443.0[(T/T_m)^{1.14} - 1]$.

DOI: 10.1103/PhysRevB.85.174104 PACS number(s): 64.10.+h, 64.70.D−, 71.15.Pd

I. INTRODUCTION

Pt is widely used as a pressure (P) standard both in static, mostly diamond anvil cell (DAC), and shockwave (SW) experiments. This is explained by the high stability of the face centered cubic (*fcc*) phase of Pt in a wide pressure range extending to at least several megabars and its chemical nonreactivity. Significant effort has been put into establishing an equation of state (EOS) for this element both by DAC[1] (up to 1 Mbar) and SW[2] (up to 6.6 Mbar) experiments. Similarly, theoretical effort led to several EOS for Pt.[3–5] These EOS also cover the range of elevated, up to 3000 K, temperatures (T). While a certain mismatch between DAC, SW, and theory does exist, the reasons for this are understood and it is not too large in general. An elaborated account of experimental and theoretical work on EOS of Pt was recently published.[5]

The use of Pt in DAC melting experiments might involve heating of Pt to extreme temperatures at high pressure. Providing the temperature of the solid-liquid transition in SW experiments is important to reduce the Hugoniot to room temperature. To our knowledge, there are five experimental papers that report melting T of Pt[6–10] at high pressure. Furthermore, there are two theoretical papers that report results of molecular dynamic (MD) simulations.[11,12] There are also several phenomenological models and thermodynamic assessments of Pt melting at high pressure (e.g.).[13] Early Pt melting experiments[6–9] were performed below 100 kbar. These measurements have been done in large volume devices and are in reasonable agreement with each other. The paper by Strong and Bundy[6] stands out somewhat. There are several revisions of their data including their own.[6,14,15] The rest of the experimental melting data below 100 kbar is self-consistent. The change of the melting T with pressure is almost linear with the dT/dP derivative about 4.2 K/kbar.[16] Considering that $T_m = 2042$ K at pressure 1 bar, then at 100 kbar the melting T is about 2450 K. Kavner and Jeanloz[10] measured in DAC the Pt melting curve in the 100–700 kbar pressure range. The temperature of melting, according to the fitted melting curve, changes in this range between 2300 and 3200 K. At the pressure of about 100 kbar, where a comparison between early melting data can be made, the melting curve fitted to the DAC data seem to be slightly lower than the early melting data.[7–9,16] However, the DAC experiment shows a point at about 110 kbar that indicates stability of solid Pt at 2500 K. It is difficult to fit the DAC data to a single melting curve under the constraint that the zero pressure melting point is 2042 K. The phenomenological theory also indicates certain problems to describe the DAC data.[13] There are two papers[11,12] that study melting of Pt by the molecular dynamics method applying the embedded-atom method to describe interatomic interaction. These papers produce rather different melting curves. Thus, at 3 Mbar the difference amounts to 2600 K. One of the papers reproduces very precisely the SW data[11] while the recent paper is in general agreement with the DAC data.[12] To our knowledge, there were no attempts to compute Pt high P melting curve from first principles. Considering the existing differences in the Pt melting data and the interest in melting of metals in general and in Pt melting in particular we decided to address the issue of high-pressure Pt melting from first principles. We decided also to check how other embedded atom models[17,18] perform when calculating Pt melting.

The paper is organized as follows. First, we describe the methods we use to calculate energies and forces in Pt. Second, we describe the molecular dynamics approach to calculate melting, namely the Z method and coexistence method. Third, we compare the calculated and experimental data. Fourth, we analyze the available data and compare it with the data calculated in this paper. This comparison allows us to provide, in our opinion, a reliable estimate of the high-pressure Pt melting curve.

II. METHODS

A. Energy and forces calculations

The calculations of the total energies were done by the projector augmented-wave (PAW) method[19] (as implemented in VASP)[20] based on the density functional theory (DFT). Exchange and correlation potentials were treated within the generalized gradient approximation (GGA).[21] The calculations were performed with the cutoff energy of 21.15 Ry, treating 5*d* and 6*s* orbitals as Pt valence states. The $2 \times 2 \times 2$ Monkhorst-Pack k-point mesh[22] is used for the supercell with 108 Pt atoms. The Brillouin-zone (BZ) integration was done by the linear tetrahedral method with Blöchl corrections.[23] The spin-orbit effect was not considered since it was found to be small.[5] The finite temperatures for the electronic structure and

force calculations were implemented within the Fermi-Dirac smearing approach.[24]

We have also performed simulations with the embedded-atom method (EAM).[18] The particular form of the applied potential is as follows:

$$U_{sc} = \epsilon \left[\sum_{i<j}^{N} \left(\frac{a}{r_{ij}} \right)^{n} - C \sum_{i}^{N} \rho_i^{1/2} \right], \quad (1)$$

where the local density ρ_i, is given by

$$\rho_i = \sum_{j}^{N} \left(\frac{a}{r_{ij}} \right)^{m}. \quad (2)$$

Here U_{sc} is the potential energy of a system of N atoms, r_{ij} is the distance between atoms i, and j, n, m, ϵ, a, and C are adjustable parameters of the potential.

We have used two sets of parameters that we call EAM1 and EAM2. The EAM1 set of parameters is introduced by Sutton and Chen.[18] It was applied successfully in a number of applications.[25,26] The EAM1 set is as follows $n = 10.0$, $m = 8.0$, $\epsilon = 0.019833$ eV, $a = 3.92$ Å, and $C = 34.408$. The EAM2 set of parameters is introduced by Luo *et al.*.[17] The EAM2 parameters are as follows: $n = 11.0$, $m = 7.0$, $\epsilon = 0.0097894$ eV, $a = 3.9163$ Å, and $C = 71.336$.

The reason we used two EAM models as well as an *ab initio* approach is simple. The two published theoretical melting curves for Pt[11,12] both applied EAM methods to describe the interactions between Pt atoms. These two curves are quite different. Therefore, we were hoping that employing two more EAM models will allow us to see whether we get a melting curve in agreement with any of the published data. Instead, we obtained another two different Pt melting curves. At this point, we decided that we cannot rely solely on the existing EAM models (we did not check them all, though; the new parametrization[27] seems very promising) and have to apply an *ab initio* method.

B. Molecular dynamics simulations

The method of molecular dynamics (MD) is a natural choice if the goal is to calculate the melting temperature. In many ways this method is similar to experiment with the major difference that experiment studies a sample while in MD method we study a model of the sample. A description of the MD method can be found elsewhere.[28] Our MD simulations have all been performed by applying periodic boundary conditions. The time step for solving the differential equations of atomic motion was equal to 4 femtoseconds ($1\ \text{fs} = 10^{-15}$) which is small considering the large atomic mass of Pt atom (195.084 a.u.). The number of time steps in our MD simulations varied depending on the task, being the lowest in the equation of state calculations at 300 K (4000 time steps) and the largest in the coexistence simulations of melting (over 1 million time steps). Most of our simulations [all of the *ab initio* MD simulations (AIMD)] were performed in the microcanonical ensemble where N (number of atoms), V (volume), and E (energy) is conserved. In some MD simulations we used the NPT ensemble.[29] The number of atoms varied from 108 atoms in AIMD simulations to around 1 million in coexistence EAM-based MD simulations. The cutoff radius in EAM simulations was set to 10 Å. The AIMD simulations have been performed using the VASP[20] package and the classical EAM simulations using the DL_POLY[30] package.

C. Z method

This method[31,32] has recently received a wide application in melting studies.[33–36] In this method one tries to determine the threshold of thermal stability. If the total energy of a system kept constant then the temperature drops to the melting temperature. Thus, the connected P-T points on the isochore form a characteristic shape similar to the letter Z. The Z method is a good alternative to the two-phase approach[37] or the coexistence method[38] because it allows one to calculate melting temperatures with a comparably modest computational effort. It is also applicable in the cases where thermodynamic integration[39] becomes prohibitively complicated, such as polyatomic systems. The method has been demonstrated to provide the melting temperature in close agreement with the two-phase method,[31] including metallic systems. If the number of atoms in the simulated system is small and the runs are comparably short the performance of this method, as well as of any statistical method, deteriorates. Therefore, a certain effort has to be put to estimate this effect. We estimate it by performing Z-method calculations for the EAM1 model with a small number of atoms and of the same duration as in the *ab initio* (108 atoms) system and comparing them to the results of coexistence simulations. This comparison (see below for details) demonstrates that the systematic error due to size effect is small as compared to the magnitude of the melting temperature and does not exceed 5% . This precision is quite sufficient to provide a sensible Pt melting curve. This is in agreement with recent estimates of the performance of the Z method.[35]

D. Coexistence method

The coexistence method, as proposed by Ladd and Woodcock,[38] consists of placing solid and liquid in the same computational cell and allowing this cell to equilibrate to the pressure and temperature of equilibrium between solid and liquid. A coexistence simulation is performed in the NVE ensemble. Note that this is different from the two-phase method, where at the end of the run, performed in the NPT ensemble, only one phase is preserved. In fact, Ladd and Woodcock, using computational cells of the size about 1000 atoms, concluded that this method is useful under conditions that the EOS of solid and liquid are well known. This is because placing solid and liquid in a box with a plain interface between eventually creates a nonhydrostatic stress when the proportions of solid and liquid during equilibration are changing. It is not important at low pressure but becomes critical at high pressure. The only way to avoid such a stress is to create the initial state at exactly the melting conditions—but, again, why would one then need to perform the coexistence simulations? When the system is large, on the order of several thousands of atoms or larger, the impact of stress becomes smaller due to the ability of the solid part to accommodate it through elastic deformation. However, in a small system this impact is severe.

Sometimes a system spends a long time equilibrating toward the melting point. In this process the ratio of solid and liquid changes building up the nonhydrostatic stress. This stress might eventually destroy the system providing the impression that the equilibrium is destroyed by a fluctuation. In fact, it could be that equilibrium has never been reached. Such a behavior has recently been reported in coexistence simulations of iron.[40]

To avoid this caveat in our coexistence simulations we create a large computational cell with Pt atoms originally arranged in the *fcc* lattice. Then, gradually heating it up we obtain the limit of superheating at this volume and transform solid into liquid. We then cool the liquid down to approximately 20% of the limit of superheating, bringing the system to approximately the melting temperature. Then, at the same temperature and pressure, we create a small, 32 000 atoms, solid sample simulated in the NPT ensemble. This solid sample is then immersed in the center of the liquid sample by removing the overlapping liquid atoms. To be on the safe side to guarantee that the solid sample will grow and establish equilibrium with the liquid, we start at a temperature which is about 200° lower. Sometimes, when we saw that the solid melts, we restarted simulations at an even lower temperature. Normally, it took about 500,000 time steps to reach equilibrium between the solid and liquid. This procedure was repeated at a number of densities to provide several points on the melting curve. More details about this approach can be found elsewhere.[41]

The coexistence simulations have been performed for the EAM1 and EAM2 models, but not by AIMD for technical reasons. First-principles treatment of such large systems is not yet possible, and small system simulation might be imprecise for the reasons explained above.

III. RESULTS AND DISCUSSION

We performed static DFT calculations at $T = 0$ K for a range of volumes to assess the performance of our method. We also performed MD simulations with the EAM1 and EAM2 models at $T = 300$ K and a range of volumes. The results of these calculations along with the most recent and carefully obtained experimental data[1] on Pt volume at ambient temperature and pressure in the range up to 900 kbar are shown in Fig. 1. We see good agreement between DFT calculated and experimental EOS. The agreement becomes better as pressure increases. The agreement in between EAM data is not as good; nevertheless it is quite reasonable. We note that the agreement between the EAM data and experiment is not surprising because most EAM models are fitted to reproduce the volume at ambient PT, cohesion energy, often bulk modulus, etc. The difference between the EAM and experimental data[1] is likely due to the difference between the experimental data sets used to fit the EAM models. Indeed, the EAM model [Eqs. (1) and (2)] has five adjustable parameters while the EOS can be fitted with a Birch-Murnaghan equation with just three parameters. Therefore, the model is sufficiently flexible to accommodate a perfect fit to experiment.

We then calculated two isochores for the *fcc* Pt, for $V = 16.0$ Å^3 and for $V = 13.08$ Å^3. We performed AIMD runs for a number of temperatures at each of the two volumes. The initial

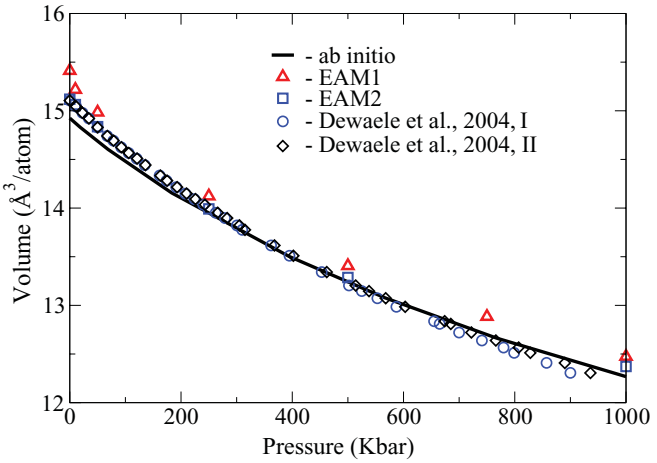

FIG. 1. (Color online) Experimental[1] data on volume of Pt at ambient temperature at a number of pressures compared to the data calculated in this work. The data calculated with a DFT-based approach is marked as *ab initio* in the legend. The *ab initio* data are obtained by static calculations at $T = 0$ K. The EAM1 and EAM2 data are obtained using embedded-atom models[17,18] and calculated with the molecular dynamics approach at $T = 300$ K.

temperature varied in the range between 4000 and 8000 K for larger volume and 8000 and 20 000 K for smaller volume. Note that due to the equipartition the average temperature becomes about half of the initial one, unless a phase transition takes place. These isochores are shown in Fig. 2. The volume 16.0 Å^3 provides a negative pressure at $T = 300$ K. This volume was chosen to verify whether our method gives a reasonable melting temperature in the range where reliable experimental data, reproduced by several techniques in several research groups in large volume high-pressure devices,[16] exists. Because on heating the pressure increases we had to start with the large volume to arrive at not too high pressure at the melting temperature. The calculated AIMD isochores are compared with the isochores calculated using thermal Pt EOS[3] (Fig. 2). One can see that the dT/dP derivative of the

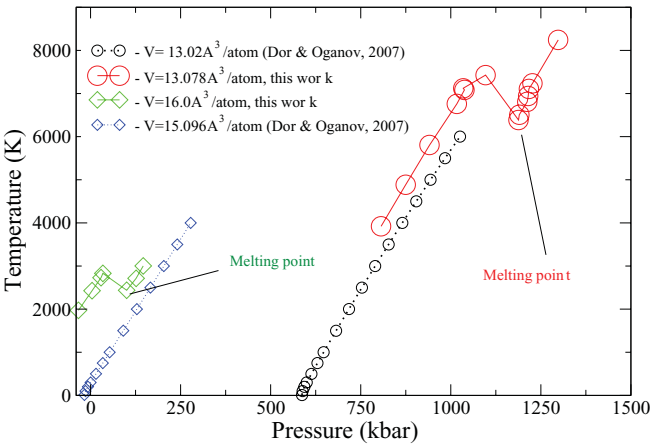

FIG. 2. (Color online) The Z isochores for volumes 16.0 Å^3/atom and 13.078 Å^3/atom (shown by solid lines with diamonds and circles correspondingly). The isochores, computed with empirical EOS,[3] are shown for comparison. The dT/dP slopes of computed and empirical isochores are close.

EOS based on the experimental data and computed from first principles are very close. This suggests that the impact of temperature is well reproduced in our AIMD simulations.

The isochores in Fig. 2 consist of two parts. One part corresponds to the solid isochore where pressure and temperature increase monotonously until they discontinuously change to rise again along the liquid part of the isochore. The lowest temperature and pressure point at the liquid part of the isochore corresponds to the point on the melting curve.

The search for the limit of superheating (T_{LS}) was arranged as follows. We started AIMD simulations with regular intervals of 1000 K and performed them for at least 4000 time steps. If at some temperature we found melting then we continued to run AIMD at the lower temperature for another 4000 time steps. If we did not see melting at the initial temperature at 1000 K lower, then we cut the interval in half and run 12 000 time steps at the initial temperature just 500 K lower than the initial temperature where the melting was discovered. Note that because the averaged temperature was about half of the initial, we scanned the temperature interval with the resolution 250 K. At low pressure the initial temperature step was 500 K which resulted in the 125-K scanning interval. Figure 3 shows the time evolution of temperature at the highest temperature point in the solid as compared to the lowest temperature in the liquid [Fig. 3(a)] and the same for pressure [Fig. 3(b)]. One can see that the pressure-temperature fluctuates around average for some time before it switches to the liquid state and starts fluctuating around the pressure in the liquid (which increases on melting) and temperature in the liquid (which decreases on melting). The inset shows that at all temperatures and both volumes the system quickly, in about 100–200 time steps looses memory of the initial state. Therefore, starting runs with different initial temperature will not affect results—effectively, every 100–200 time steps we start from a different initial state. Comparing the runs at close temperatures we conclude that if the duration of run is important it will result in a smaller error than the scanning temperature steps, that is, 125 and 250 K at large and low volume correspondingly. In our experience with large systems[31] a temperature change on the level of 1% allows one to shorten the run duration from 1 million to 10 000 time steps to observe melting.

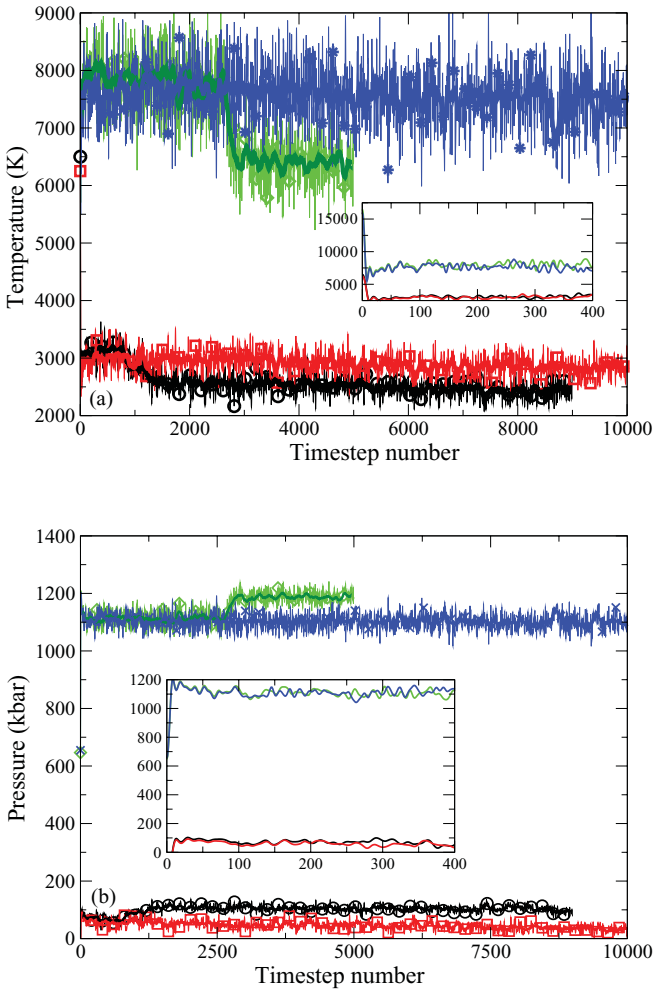

FIG. 3. (Color online) Temperature (a) and pressure (b) time history for the MD runs performed at $V = 16.00$ Å^3/atom (circles and boxes) and $V = 13.078$ Å^3/atom (stars and diamonds). Insets show the first 400 time steps. The running averages over 100 time steps are shown by thick solid curves. The runs that started at the $T_{\text{start}} = 6500$ K (circles) and $T_{\text{start}} = 16\ 500$ K (diamonds) exhibit discontinuous behavior characteristic of melting. A similar change can be seen for pressure. For the $T_{\text{start}} = 6250$ K (boxes) and $T_{\text{start}} = 16\ 000$ K (stars) no similar changes can be seen; the system remains metastably in the solid state.

The melting data obtained with the coexistence method using the two EAM models and with the Z method using AIMD is shown in Fig. 4 along with the published data on Pt melting. One can immediately see that EAM methods do not provide sensible constraints on the Pt melting curve. For example, at a pressure of 750 kbar, computed melting temperatures vary in the range 3000–6000 K. The lowest EAM melting curve[12] and the DAC melting curve[10] seem to converge in the high-pressure range, however, it looks like that if the DAC curve would be extrapolated it would be below the lowest EAM melting curve. Thus, the lowest Pt melting curve is obtained in DAC experiments. We note that this is similar to the experience for a number of substances, such as Fe, Mo, Ta, MgO, where the experimental melting curves are normally below those computed from first principles as well as those measured in shockwave experiments, at the same time shockwave data and first-principles melting curves are in reasonable agreement with each other. Therefore, such a disagreement is not surprising—on the contrary, it is expected.

The first-principles data on Pt melting are in excellent agreement with the experimental data obtained in large-volume pressure devices,[6,8] particularly with the data by Mitra *et al.*.[8] The AIMD melting point at the pressure of 100.28 kbar is equal to 2437.1 K while according to Mitra *et al.*[8] the melting temperature at this pressure is equal to 2462 K. The high-pressure AIMD melting point is at 1188 kbar and 6387 K. This temperature is just slightly lower than the temperature according to the extrapolation in the paper by Mitra *et al.*.[8] In addition, their extrapolation is in very good agreement with the EAM melting curve computed with the Sutton-Chen EAM model[18] parametrized originally by Sutton and Chen. Considering that the method for computing low- and high-pressure points are exactly the same, we expect the same accuracy and reliability of the computed data. It is very unlikely that the excellent agreement between the reliable experimental

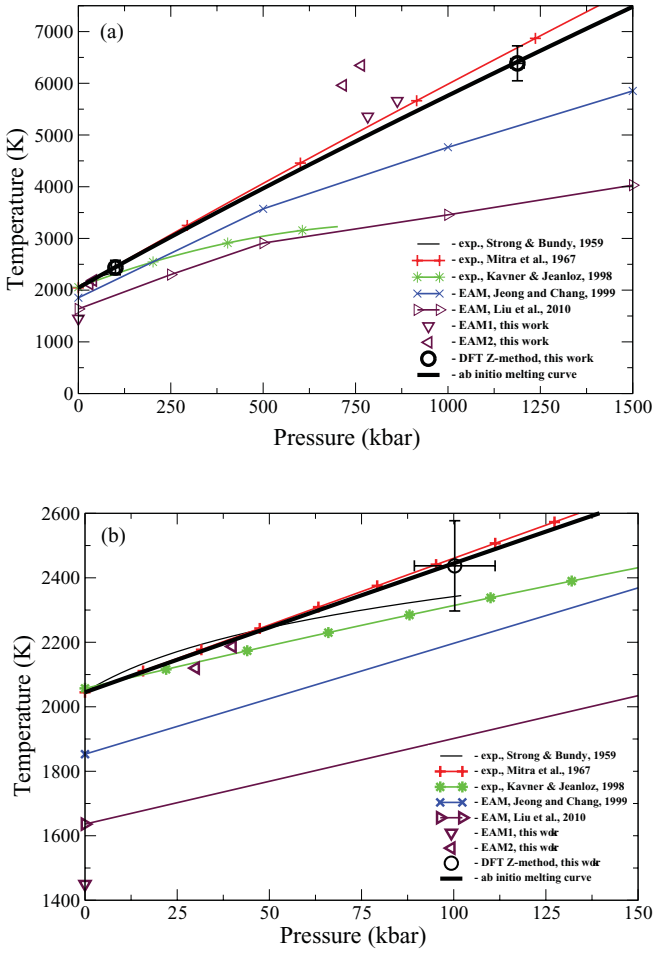

FIG. 4. (Color online) Melting data from several sources in the pressures range 0–1500 Kbar (a) and 0-150 Kbar (b). There is a remarkable agreement between the data calculated in this work from first principles (circles and thick black solid curve) and those measured by Mitra, Decker, and Vanfleet.[8] The red curve marked with pluses is the extrapolation of the Mitra *et al.* experimental data using their original parametrization of the Simon equation. The original parametrization of the Sutton Chen model by Sutton and Chen[18] (EAM1) is also very close to the *ab initio* data obtained in this work at high pressure (a).

melting data by Mitra *et al.*,[8] its extrapolation to high pressure, and computed EAM1 and AIMD data is fortuitous. The mere probability of such a coincidence is nearly zero. Therefore, we conclude that our method does provide us an important constraint on the melting curve of Pt.

The experimental data in Mitra *et al.*[8] were fitted using the Simon equation,[42]

$$P_m/A = (T_m/T_{m,0})^c - 1 \tag{3}$$

where P_m and T_m are the pressure and temperature at melting and $T_{m,0}$ is the melting temperature at atmospheric pressure. Several theoretical estimates for the parameters c have been proposed in early papers.[43–45] Since then, the Simon equation has been investigated and various improvements have been suggested.[46,47] However, for our purposes, namely to correct the original equation using new AIMD data, we will use the original Simon equation. Considering that we have got excellent agreement with the Mitra *et al.*[8] data we decided to keep the original parameter A that defines the pressure scale and just change the parameter c so that the Pt melting curve would go through the computed AIMD high-pressure melting point. The newly parametrized Simon equation[42] for the Pt melting curve is as follows:

$$P_m = 443 \times (T_m/2042.0)^{1.14} - 1, \tag{4}$$

where the P_m will be computed in kilobars. The original[42] c parameter is equal to 1.1; a slight change of this parameter is sufficient to describe both new computed and old experimental data.

The shockwave data on Pt exhibit a discontinuity at pressures between 3 and 4 Mbar. The T_m in this pressure range is between 11 000 and 13 000 K. The T_m extrapolated with the data from DAC would result in a T_m below 5000 K, which is unusually low for melting of metals in shockwave experiments above 3 Mbar.

It is of interest how the structure of the liquid changes along the melting curve. Figure 5 shows the radial distribution functions computed at the low and high AIMD melting points (Fig. 4). The RDFs are computed as the ratio of local and average density,

$$g(r) = \rho(r)/\rho_0. \tag{5}$$

Knowing $g(r)$, one can compute a running average coordination number CN by integrating $g(r)$:

$$CN(r) = 4\pi \int g(r) r^2 dr. \tag{6}$$

The low- and high-pressure CN are provided in Fig. 5. We see that the RDF at high P is broader and the first peak is lower than the first peak of RDF at low pressure. This is likely due to higher temperature. The CNs, however, are quite identical.

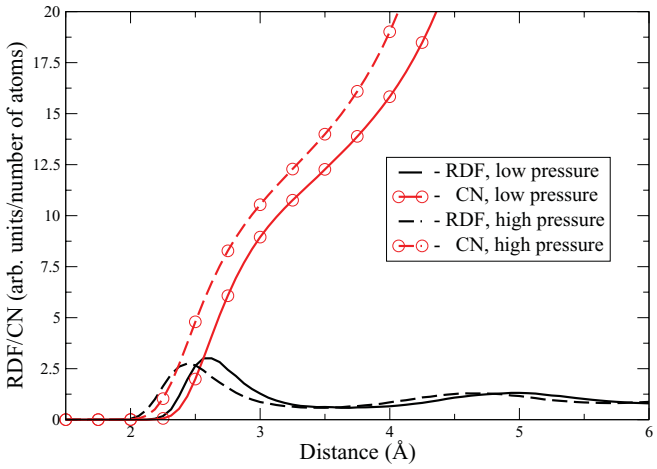

FIG. 5. (Color online) Structure of the liquid calculated by AIMD at two melting points (Fig. 2). A comparison of the running coordination numbers at these pressures demonstrates quite similar structures where the only change is a shortening of distances. The first neighbor shell is somewhat widened at the high pressure point due to the higher temperature.

This suggests that the structure of liquid Pt remains the same along the melting curve, except that the distances become shorter. We know from the Clausius-Clapeyron equation that

$$dT/dP = \Delta S/\Delta V. \quad (7)$$

The slope of the Pt melting curve is nearly constant up to 4 Mbar. The liquid structure, being the same along the melting curve (Fig. 5) suggests that the entropy of liquid, and, therefore, the entropy change on melting remain mostly the same along the melting curve. This suggests that the ΔV on melting does not change much being about 7% at low pressure.[8]

The AIMD calculations are expensive. The 1000 time steps AIMD run for 108 Pt atoms with 10 valence electrons and k-mesh $2 \times 2 \times 2$ require about 70 h with 64 CPUs. Considering that some PT points are computed for 12 000 time steps and there are about 30 such points, the total CPU time spent to compute these two melting points is more than 1 000 000 h of computer time. The advantage of the Z method is that all these calculations can be run separately with a very high parallel efficiency. Even though we computed just two melting points, they allow one to tell that (a) the computed data is reliable and (b) the Pt melting temperature is much higher than implied by the DAC measurements.

The failure of several EAM models to provide a correct melting curve is obvious (Fig. 4). In our experience[48,49] an EAM model fails if the configurations that are used to fit such a model are mostly symmetric. When the set of configurations includes liquid configurations, the EAM model correctly reproduces the energy difference between solid and liquid and, thus, correct melting curve. Therefore, the poor performance of three of the EAM models in this work is solely due to their poor parametrization. When relevant data is included in the parametrization[48–50] the quality and reliability of results becomes comparable to or even better than the precision of *ab initio* models.

IV. CONCLUSIONS

We computed the Pt melting curve from first principles. This curve is in remarkable agreement with low-pressure melting data. The curve is very close to the extrapolation of the experimental data with the Simon equation. One of the investigated EAM models is in agreement with the *ab initio* melting point at high pressure. Unfortunately, the high-pressure Pt melting curve measured in DAC is yet another example where the *ab initio* data is sharply different from the DAC experiment. Apparently, a serious effort has to be made to find out the reasons for this discrepancy. The EAM models have to be parametrized using *ab initio* data on solid and liquid phases.

ACKNOWLEDGMENTS

Computations were performed using the facilities of the National Supercomputer Center in Linköping. P. I. Dorogokupets provided us with the tabulated data for his EOS.[3] Discussions with A. Goncharov and V. Prakapenka were useful. A.B. thanks the Swedish Research Council (VR) and Göran Gustafsson Foundation (GGS) for financial support.

[1] A. Dewaele, P. Loubeyre, and M. Mezouar, Phys. Rev. B **70**, 094112 (2004).
[2] N. C. Holmes, J. A. Moriarty, G. R. Gathers, and W. J. Nellis, J. Appl. Phys. **66**, 2962 (1989).
[3] P. I. Dorogokupets and A. R. Oganov, Phys. Rev. B **75**, 024115 (2007).
[4] M. Matsui, E. Ito, T. Katsura, D. Yamazaki, T. Yoshino, A. Yokoyama, and K. Funakoshi, J. Appl. Phys. **105**, 013505 (2009).
[5] T. Sun, K. Umemoto, Z. Wu, J.-C. Zheng, and R. M. Wentzcovitch, Phys. Rev. B **78**, 024304 (2008).
[6] H. M. Strong and F. P. Bundy, Phys. Rev. **115**, 278 (1959).
[7] N. S. Fateeva, L. F. Vereshchagin, and V. S. Kolotygin, Dokl. Akad. Nauk SSSR **152**, 88 (1963).
[8] N. R. Mitra, D. L. Decker, and H. B. Vanfleet, Phys. Rev. **161**, 613 (1967).
[9] L. F. Vereshchagin and N. S. Fateeva, Sov. Phys. JETP USSR **28**, 597 (1969).
[10] A. Kavner and R. Jeanloz, J. Appl. Phys. **83**, 7553 (1998).
[11] J.-W. Jeong and K. J. Chang, J. Phys.: Condens. Matter **11**, 3799 (1999).
[12] Z.-L. Liu, J.- Hui Yang, Z.-G. Zhao, L.-C. Cai, and F.-Q. Jing, Phys. Lett. A **374**, 1579 (2010).
[13] Z. Wang, P. Lazor, and S. K. Saxena, Phys. B **293**, 408 (2001).
[14] L. Liu and W. Bassett, *Elements, Oxides, Silicates: High Pressure Phases with Implications for the Earth's Interior* (Oxford University Press, New York, 1986).
[15] D. A. Young, *Phase Diagrams of the Elements* (University of California Press, Berkeley, 1995), p. 291.
[16] E. Y. Tonkov, *High Pressure Phase Transformations: A Handbook*, Vol. 2 (Gordon and Breach Science Publishers, Philadelphia, 1992), p. 642.
[17] S.-N. Luo, T. J. Ahrens, T. Cagin, A. Strachan, W. A. Goddard III, and D. C. Swift, Phys. Rev. B **68**, 134206 (2003).
[18] A. P. Sutton and J. Chen, Philos. Mag. Lett. **61**, 139 (1990).
[19] P. E. Blöchl, Phys. Rev. B **50**, 17953 (1994).
[20] G. Kresse and J. Furthmüller, Comput. Mater. Sci. **6**, 15 (1996); Phys. Rev. B **54**, 11169 (1996); G. Kresse and D. Joubert, *ibid.* **59**, 1758 (1999).
[21] Y. Wang and J. P. Perdew, Phys. Rev. B **44**, 13298 (1991); J. P. Perdew, J. A. Chevary, S. H. Vosko, K. A. Jackson, M. R. Pederson, D. J. Singh, and C. Fiolhais, *ibid.* **46**, 6671 (1992).
[22] H. J. Monkhorst and J. D. Pack, Phys. Rev. B **13**, 5188 (1976).
[23] P. E. Blöchl, O. Jepsen, and O. K. Andersen, Phys. Rev. B **49**, 16223 (1994).
[24] N. D. Mermin, Phys. Rev. **137**, A1441 (1965).
[25] K. Kayhani, K. Mirabbaszadech, P. Nayebi, and Mohandesi, Appl. Surf. Sci. **256**, 6982 (2010).
[26] S.-H. Lee, S. S. Han, J. K. Kang, J. H. Ryu, and H. M. Lee, Surf. Sci. **602**, 1433 (2008).
[27] J. H. Li, Y. Kong, H. B. Guo, S. H. Liang, and B. X. Liu, Phys. Rev. B **76**, 104101 (2007).

[28] J. M. Haile, *Molecular Dynamics Simulation: Elementary Methods* (John Wiley & Sons, New York, 1997).
[29] G. Martyna, M. Tuckerman, D. Tobias, and M. Klein, Mol. Phys. **87**, 1117 (1966).
[30] I. T. Todorov, W. Smith, K. Trachenko, and M. T. Dove, J. Mater. Chem. **16**, 1911 (2006).
[31] A. B. Belonoshko, N. V. Skorodumova, A. Rosengren, and B. Johansson, Phys. Rev. B **73**, 012201 (2006).
[32] A. B. Belonoshko, L. Burakovsky, S. P. Chen, B. Johansson, A. S. Mikhaylushkin, D. L. Preston, S. I. Simak, and D. C. Swift, Phys. Rev. Lett. **100**, 135701 (2008); L. Burakovsky, S.-P. Chen, D. L. Preston, A. B. Belonoshko, A. Rosengren, A. S. Mikhaylushkin, S. I. Simak, and J. A. Moriarty, *ibid.* **104**, 255702 (2010).
[33] J. Bouchet, F. Bottin, G. Jomard, and G. Zerah, Phys. Rev. B **80**, 094102 (2009).
[34] A. R. Finney and P. M. Rodger, Phys. Chem. Chem. Phys. **13**, 19979 (2011).
[35] D. Alfe, C. Cazorla, and M. J. Gillan, J. Chem. Phys. **135**, 024102 (2011).
[36] J. A. Moriarty, R. Q. Hood, and L. H. Yang, Phys. Rev. Lett. **108**, 036401 (2012).
[37] A. B. Belonoshko, Geochim. Cosmochim. Acta **58**, 4039 (1994).
[38] A. J. C. Ladd and L. V. Woodcock, Mol. Phys. **36**, 611 (1978); J. R. Morris, C. Z. Wang, K. M. Ho, and C. T. Chan, Phys. Rev. B **49**, 3109 (1994).
[39] D. Frenkel and A. J. C. Ladd, J. Chem. Phys. **81**, 3188 (1984).
[40] D. Alfe, Phys. Rev. B **79**, 060101 (2009).
[41] A. B. Belonoshko, Phys. Rev. B **78**, 174109 (2008).
[42] F. Simon and G. Glatzel, Z. Anorg. Allg. Chem. **178**, 309 (1929).
[43] J. J. Gilvarry, Phys. Rev. **102**, 308 (1956).
[44] J. J. Gilvarry, Phys. Rev. **102**, 325 (1956).
[45] D. L. Decker and H. B. Vanfleet, Phys. Rev. **138**, A129 (1965).
[46] H. Schlosser, P. Vinet, and J. Ferrante, Phys. Rev. B **40**, 5929 (1989).
[47] M. Z. Faizullin and V. P. Skripov, High Temp. **45**, 621 (2007).
[48] A. B. Belonoshko, R. Ahuja, O. Eriksson, and B. Johansson, Phys. Rev. B **61**, 3838 (2000).
[49] A. B. Belonoshko, R. Ahuja, and B. Johansson, Phys. Rev. Lett. **84**, 3638 (2000).
[50] A. B. Belonoshko, R. Ahuja, and B. Johansson, Nature (London) **424**, 1032 (2003).